International Journal of Power Electronics and Drive System (IJPEDS)
Vol. 6, No. 4, December 2015, pp. 759~771
ISSN: 2088-8694

The Camparison of Harmonic Distortion Self-Excited Induction Generator with Isolated Synchronous Generator Under Non-linear Loads

Refdinal Nazir[1], Krismadinata[2], Rizka Amalia[1]
[1] Electrical Engineering Department, Andalas University, Indonesia
[2] Electrical Engineering Department, Padang State University, Indonesia

Article Info

Article history:

Received Jul 31, 2015
Revised Nov 18, 2015
Accepted Nov 29, 2015

Keyword:

Harmonic Distortion
Non-linear Load
SEIG
Synchronous Generator
Total Harmonic Distortion

ABSTRACT

In this paper, the harmonic distortion for Self-Excited Induction Generator (SEIG) and an isolated synchronous generator (ISG) under non-linear load during steady state conditions are analyzed. The voltage and current harmonics distortion for both generators are calculated using the transfer function method in frequency domain for SEIG and phasor diagram method for ISG. This analysis is done independently one by one component for all harmonic components appear. The analysis results for both generators are verified to the laboratory test results. For loading with the same non-linear load to both generators, the harmonics distortion on the stator windings of SEIG was smaller than compare ISG. In addition, the harmonic distortion effects on other loads connected to PCC point of SEIG was lower than the other loads connected to ISG.

Corresponding Author:

Refdinal Nazir,
Departement of Electrical Engineering,
Andalas University,
Limau Manis Campus, Padang 25163, Indonesia.
E-mail: refdinalnazir@yahoo.co.id

1. INTRODUCTION

Currently, the applications of Self-Excited Induction generator (SEIG) are more common in small-scale power plants using renewable energy sources, including: wind, mini/microhydro, tidal wave, biomass, biogas, etc. [1],[2]. Meanwhile, the isolated synchronous generators (ISG) are widely applied in diesel electric generating sets (Genset). In its application, the two generators are often employed to drive non-linear loads, including: uninterruptible power supply (UPS), variable frequency drives (VFD), switched mode power supply (SMPS), energy-saving lamp (ESL), etc. The imposition of generator with non-linear loads will have an impact on the generation of harmonic currents and voltages distortion. The generation of harmonic currents in the generator has adverse effects upon its performance. It can give the effect of decreasing efficiency, heating and reducing the life time of the generator [3]-[5]. Harmonic distortion of the voltage generator will be able to create a harmonic disturbance to other loads, which are connected in parallel to the same source.

The levels of harmonic distortion incurred due the employed of non-linear loads on SEIG and ISG will be different. This level of harmonic distortion is influenced by the equivalent circuit structure of the generator and its parameters. Generators for Genset usually have higher the reactance than the distribution transformers on utility networks [3]. Consequently, the rate for the harmonic distribution of the generator voltage is higher than the utility source, if both sources operate with the same non-linear load. The equivalent circuit structure of SEIG has the combination between magnetization inductance and excitation capacitance that can reduce the distortion harmonics. In the previous study, analysis of harmonic propagation on SEIG when its is loaded by non-linear load [6]. The results showed that SEIG rejects the high order harmonics and attenuates low order harmonics currents on its stator windings; consequently THD_I is low relatively on the stator windings.

In this paper, the current and voltage harmonic distortion for SEIG and ISG under non-linear loads during steady state conditions are analysed. The analysis result of harmonic distortion for two generators is compared in order to show the impact of non-linear loads on the both generator and other loads connected to the same sources. This paper is organized into 7 sections. In section 2, the system description of proposed system is presented. Modeling and analysis for SEIG with non-linear load is discussed in section 3. In section 4, the harmonics distortion of ISG under non-linear loads is discussed. The experimental set-up is explained in section 5. The section 6 discusses the results and its analysis. Conclusions are presented in section 7.

2. SYSTEM DESCRIPTION

The configuration of studied system consists of a generator, non-linear loads, and other loads that are linearly, as shown by Figure 1. In this system, Variable Fequency Drive (VFD) and Energy-Saving Lamp (ESL) are applied as non-linear load and resistor is employed as the other load. The harmonic currents, I_h, flow from the non-linear loads to the generator and other load, R_L. In the SEIG, the harmonic currents flow to the stator windings and the excitation capacitors that are low impedance to high frequencies, while the harmonic currents flow only to the stator windings in the ISG. Furthermore, the both generators also produce the small harmonic of voltages due to the imperfection of its construction.

Figure 1a shows the configuration of studied system using SEIG. As shown in this figure, SEIG is constructed by an induction machine and an excitation capacitor. $\boldsymbol{Z}_{im}$ is the internal impedance of induction machine, which will be determined in next section. Meanwhile, the configuration of studied system using an isolated synchronous generator is shown by Figure 1b**.** This study uses a salient pole synchronous generator, so the synchronous impedance $\boldsymbol{Z}_s$ is constructed by a direct synchronous reactance Z_d and quadrature synchronous reactance Z_q [7].

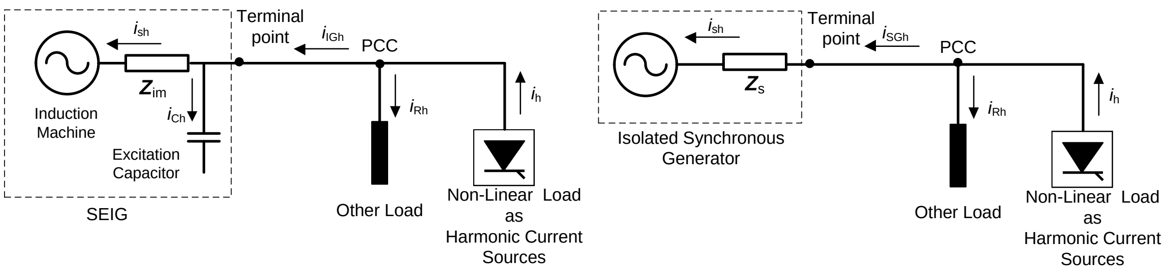

a. studied system using SEIG b. studied system using ISG

Figure 1. The configuration of studied system

3. HARMONIC ANALYSIS OF SEIG

The single-phase equivalent circuit of SEIG with non-linear load is shown in Figure 2. In this circuit, the non-linear loads are modeled as a current fundamental component $\boldsymbol{I}_1$, and harmonic current sources: $\boldsymbol{I}_2$, $\boldsymbol{I}_3$, ..., $\boldsymbol{I}_n$ [8]. Whereas, SEIG model is constructed by the circuit of induction machine and the excitation capacitor C_e. Where R_s, L_s, $R_r^{'}$, and $L_r^{'}$ are the stator resistance, stator leakage inductance, rotor resistance, and rotor leakage inductance respectively. E_g and σ are the voltage of air gap and slip. R_L is the other load, which is the linear load connected at PCC point.

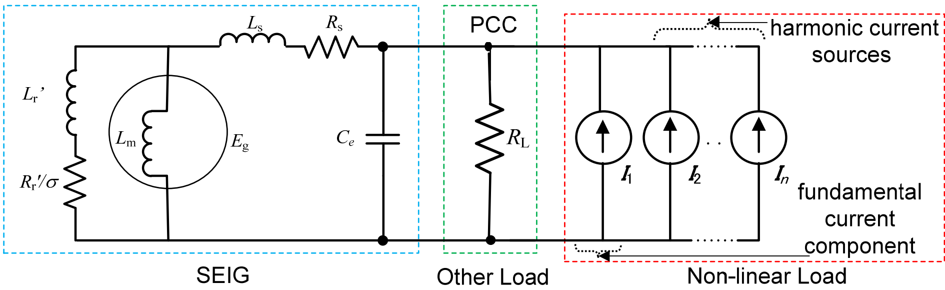

Figure 2. Single-phase equivalent circuit of studied system using SEIG

The analysis is conducted using the single-phase equivalent circuit as shown in Figure 2. This circuit contains non-linear load as *n* unit's current sources and SEIG as voltage sources. Besides that, the other load as linear load R_L is connected in parallel with the non-linear load at PCC point. The response of each source to the circuit of machine stators and other load are evaluated separately. The total response can be solved from the summation of the current response of each source and voltage response.

3.1. Current Sources Response

For current sources response, the analysis is performed by considering one current source, I_h. Meanwhile, the other current sources and voltage source are replaced respectively with an open circuit and internal impedance of SEIG. Figure 3a shows the equivalent circuit for one harmonic current source. In this analysis, the equivalent circuit is expressed in the domain frequency ω. In this condition, $\omega = h\omega_1$, where h and ω_1 are number of harmonics and fundamental frequency respectively. The correlation between the currents is produced by non-linear load $\boldsymbol{I}$(h), the other load currents $\boldsymbol{I}_L$(h), and the current in to induction generator $\boldsymbol{I}_{IG}$(h) is expressed as,

$$\boldsymbol{I}_{IG}(h) = \boldsymbol{I}(h) - \boldsymbol{I}_L(h) \tag{1}$$

$$\text{where, } \boldsymbol{I}(h) = \frac{\mathbf{V}_t(h)}{R_L}$$

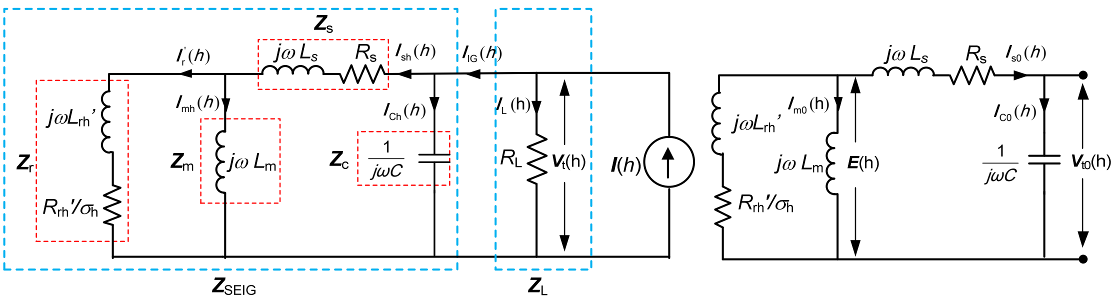

a. one current source response b. no-load response

Figure 3. SEIG equivalent circuit for analysis

From the equivalent circuit of Figure 3, the induction machine impedance, $\boldsymbol{Z}_{im}$, can be expressed as,

$$\boldsymbol{Z}_{im} = \left\{ \left(\frac{R'_{rh}}{\sigma_h} + j\omega L'_{rh} \right) // \left(j\omega L_m \right) \right\} + \left(R_s + j\omega L_s \right) \tag{2}$$

where, a slip, σ_h, is defined as,

$$\sigma_{\rm h} = \frac{h\omega_1 - \omega_{\rm r}}{h\omega_1} \tag{3}$$

If $L_{\rm mr} = \left(L_{\rm m} + L'_{\rm rh}\right)$ and $R'_{\rm r\sigma} = R'_{\rm r}/\sigma_{\rm h}$, then Eq. 5 can be solved as,

$$\boldsymbol{Z}_{\rm im} = \frac{R'_{\rm r\sigma}R_{\rm s} - \omega^2\left(L_{\rm m}L'_{\rm rh} + L_{\rm s}L_{\rm mr}\right) + j\omega\left(R'_{\rm r\sigma}L_{\rm s} + L_{\rm m}R'_{\rm r\sigma} + R_{\rm s}L_{\rm mr}\right)}{R'_{\rm r\sigma} + j\omega L_{\rm mr}} \tag{4}$$

The transfer function $\boldsymbol{T}_{\rm s}(jh\omega_1)$ or $\boldsymbol{T}_{\rm s}(h)$ as a current gain between the stator current $\boldsymbol{I}_s$(h) and the input currents of SEIG $\boldsymbol{I}_{\rm IG}$(h) can be written as,

$$\boldsymbol{T}_{\rm s}({\rm h}) = \frac{\boldsymbol{I}_{\rm s}({\rm h})}{\boldsymbol{I}_{\rm IG}({\rm h})} = \frac{\boldsymbol{Z}_{\rm C}}{\boldsymbol{Z}_{\rm im} + \boldsymbol{Z}_{\rm C}} \tag{5}$$

Or

$$\boldsymbol{T}_{\rm s}({\rm h}) = \frac{R'_{\rm r\sigma} + jh\omega_1 L_{\rm mr}}{R'_{\rm r\sigma} - h^2\omega_1^2\left(R'_{\rm r\sigma}L_{\rm m}C_{\rm e} + R'_{\rm r\sigma}L_{\rm s}C_{\rm e} + R_{\rm s}L_{\rm mr}C_{\rm e}\right) + j\left\{h\omega_1\left(R'_{\rm r\sigma}R_{\rm s}C_{\rm e} + L_{\rm mr}\right) - h^3\omega_1^3\left(L_{\rm s}L_{\rm mr}C_{\rm e} + L_{\rm m}L'_{\rm r}C_{\rm e}\right)\right\}} \tag{6}$$

Furthermore, the stator currents $\boldsymbol{I}_{\rm s}(h)$ can be solved using the following equations:

$$\boldsymbol{I}_{\rm sh}(h) = \boldsymbol{T}_{\rm s}(h)\boldsymbol{I}_{\rm IG}(h) \tag{7}$$

The magnetizing current $\boldsymbol{I}_{\rm m}(h)$ can be calculated as,

$$\boldsymbol{I}_{\rm mh}({\rm h}) = \frac{R'_{\rm r\sigma} + jh\omega_1 L'_{\rm rh}}{R'_{\rm r\sigma} + jh\omega_1 L_{\rm mr}}\boldsymbol{I}_{\rm s}({\rm h}) \tag{8}$$

3.2. No-Load Response

No-load response is used to obtain the excitation current flowing in the stator windings to generate a generator voltage. This can be done through direct measurement of the stator current at no-load conditions. At this measurement, the value of excitation capacitor is kept constant, while the rotor speed is set to obtain the fundamental frequency of 50 Hz. As shown in Figure 3b, the stator currents at no-load conditions $\boldsymbol{I}_{\rm s0}$(h) is equal to the current of excitation capacitor $\boldsymbol{I}_{\rm c}$(h) or the magnetization current -$\boldsymbol{I}_{\rm m0}$(h). Assumed, the current flowing in the rotor circuit is negligible. The harmonic components appearing at no-load conditions are caused by the inherent nature of the generator.

3.3. Total Response

The currents flowing in the SEIG circuit are obtained from the total response of the current sources and no-load response, as shown by the following equation:

$$\boldsymbol{I}_{\rm s}({\rm h}) = \boldsymbol{I}_{\rm s0}(h) - \boldsymbol{I}_{\rm sh}({\rm h}); \boldsymbol{I}_{\rm m}({\rm h}) = \boldsymbol{I}_{\rm m0}({\rm h}) + \boldsymbol{I}_{\rm mh}({\rm h}) \tag{9}$$

The terminal votage of SEIG in the harmonic distortion can be solved as,

$$\boldsymbol{V}_{\rm t}(h) = \boldsymbol{E}(h) - \boldsymbol{I}_{\rm s}({\rm h})(R_{\rm s} + jX_{\rm s}) \tag{10}$$

where, E(h) is the air gap voltage that its is determined as (see Figure 3b),

$$\boldsymbol{E}({\rm h}) = \boldsymbol{V}_{\rm t0}({\rm h}) + \boldsymbol{I}_{\rm s0}({\rm h})(R_{\rm s} + jX_{\rm s}) \tag{11}$$

The total rms of magnetizing current I_m(rms) can be calculated as [8],

$$I_m(\text{rms}) = \sqrt{\sum_{h=1}^{n} I_m^2(h)} \tag{12}$$

The value of magnetizing inductance L_m applied in this section depends on the value of magnetizing current $\boldsymbol{I}_m$, which its variation is obtained from the experimental results. In addition, the values of R_{rh}' and L_{rh}' for different harmonic orders is solved using the block rotor test [6],[9],[10]. The experimental results are resolved through curve fitting for a number of data that obtained from the experimental test. This method is implemented with *polyfit* statement in MATLAB, so R_r'(h), L_r'(h) and $L_m(I_m)$ are obtained as:

$$R_r\text{'}(h) = c_1h^4 + c_2h^3 + c_3h^2 + c_4h + c_5\ ;\ L_r\text{'}(h) = d_1h^4 + d_2h^3 + d_3h^2 + d_4h + d_5 \tag{13}$$

$$L_m(I_m) = e_1I_m^{\ 3} + e_2I_m^{\ 2} + e_3\ I_m + e_4 \tag{14}$$

where, *c,d* & *e* are a polynomial coeficient that its values are given in Appendix. In this analysis, Eq. 13 & Eq. 14 are applied for harmonic orders till 20th, and can be assumed a constant for harmonic orders above 20th.

4. HARMONIC ANALYSIS OF ISG

The analysis of harmonics distortion for ISG is conducted using the equivalent circuit and phasor diagram that shown by Figure 4 & 5. As shown in Figure 4, the non-linear load is modelled as a fundamental current component and harmonic current sources. Another load current that is connected to the same PCC will also be contaminated by harmonic components $\boldsymbol{I}_L$(h). Because this study uses the salient pole synchronous generator, the synchronous reactance X_s is split into the reactance in the direct axis X_d and the reactance in the quadrature axis X_q, as shown in Figure 5a [7],[11]. Likewise, the current flows through the stator windings are also decomposed into the current in the direct axis I_{sd} and the current in the quadrature axis I_{sq}.

To analyze the response of harmonic current sources, each order-by-order harmonic component is evaluated using an equivalent circuit as shown in Figure 5a. Here, $\boldsymbol{E}$(h) is the harmonic voltage distortion of the air gap, which is the innate nature of the generator. $\boldsymbol{E}$(h) can be obtained from no-load test results. The correlation between the currents is produced by non-linear load $\boldsymbol{I}$(h), the other load currents $\boldsymbol{I}_L$(h), and the stator current $\boldsymbol{I}_s$(h) for h^{th} order component is given as,

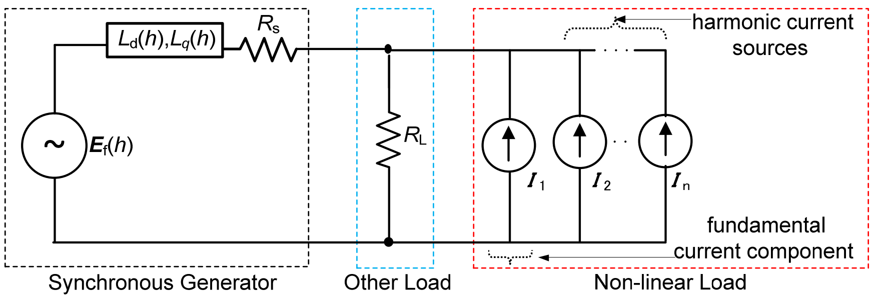

Figure 4. Equivalent circuit of studied system using ISG

$$\boldsymbol{I}_s(h) = \boldsymbol{I}(h) - \boldsymbol{I}_L(h) \tag{15}$$

where, the other load current can be calculated as,

$$\boldsymbol{I}_L(h) = \frac{\boldsymbol{V}_t(h)}{R_L} \tag{16}$$

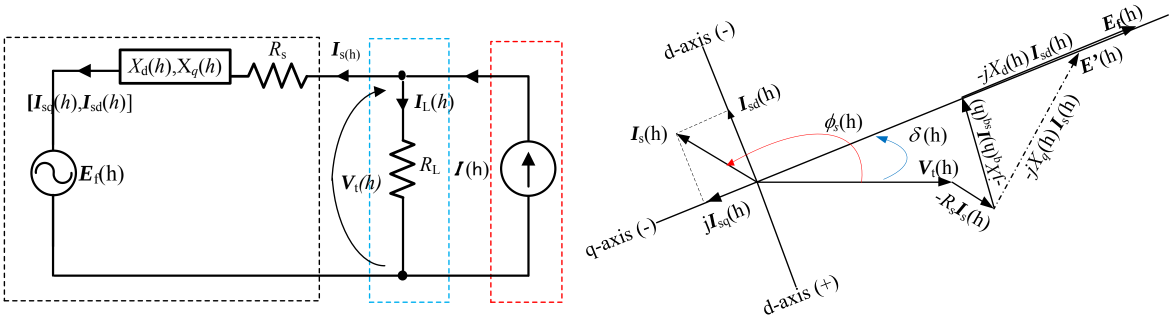

a. simplified equivalent circuit b. phasor diagram

Figure 5. Simplified equivalent circuit and phasor diagram of ISG for h^{th} harmonic order of non-linear load

The phasor diagram of synchronous generator for h^{th} harmonic component of non-linear load is given in Figure 5b. To determine the phase angle δ(h), the following relationship is used,

$$\boldsymbol{E'}(h) = \boldsymbol{V}_t(h) - R_s\boldsymbol{I}_s(h) - jX_q(h)\boldsymbol{I}_s(h) \qquad (17)$$

where, $X_q(h) = jh\omega_1 L_q(h)$ and $X_d(h) = jh\omega_1 L_d(h)$

Here, $\boldsymbol{E'}$(h) in phasor form can be written as,

$$\boldsymbol{E}'(h) = \left|\boldsymbol{E}'(h)\right| \angle\delta \qquad (18)$$

The current source harmonic in terms d-axis and q-axis can be presented as,

$$I_{sd}(h) = I_s(h)\sin\left\{\phi_s(h) - 90^0 - \delta(h)\right\} \qquad (19)$$

$$I_{sq}(h) = I_s(h)\cos\left\{\phi_s(h) - 90^0 - \delta(h)\right\} \qquad (20)$$

Furthermore, the terminal voltage equation can be written as:

$$\boldsymbol{E}_f(h) = \boldsymbol{V}_t(h) - R_s\boldsymbol{I}_s(h) - jX_q(h)\boldsymbol{I}_{sq}(h) - jX_d(h)\boldsymbol{I}_{sd}(h) \qquad (21)$$

The harmonic component of terminal voltage can be solved as:

$$\boldsymbol{V}_t(h) = \boldsymbol{E}_f(h) + R_s\boldsymbol{I}_s(h) + jX_q(h)\boldsymbol{I}_{sq}(h) - jX_d(h)\boldsymbol{I}_{sd}(h), \quad \text{for } h = 2, 3, 4....... \qquad (22)$$

where $\boldsymbol{E}_f(h)$ is congenital harmonic component of the induction voltage, which is determined through the no load test.

The influence of harmonics on the direct inductance, L_d(h), and the quadrature inductance, L_q(h), are measured based on the method meansurement in several literature [11],[12]. The variation of L_d and L_q with the harmornic orders h is resolved through curve fitting for a number of data that obtained from the experimental test. This method is implemented with *polyfit* statement in MATLAB, so L_d (h) and L_q (h) is obtained as:

$$L_d(h) = k_1h^4 + k_2h^3 + k_3h^2 + k_4;\ L_q(h) = m_1h^4 + m_2h^3 + m_3h^2 + m_4 \qquad (23)$$

where, *k* & *m* are polynomial coeficient, which its values are given in **Appendix**. In this analysis, Eq. 23 is used for harmonic orders till 20^{th}, and can be assumed a constant for harmonic orders above 20^{th}.

5. EXPERIMENTAL SETUP

The analysis results of proposed models are validated through comparisons between analysis and experimental test results. Figure 6 shows the testing circuit for all the proposed configuration system. The experimental test contains two steps, as shown in Figure 6. The first step is performed the testing of SEIG under non-linear loads. The testing of ISG under non-linear loads is done on the second step. For all test conditions, the frequency fundamental for both the generator is set at its nominal value (50 Hz) by adjusting the rotor speed.

This test uses two generators using the machines with the same capacity, namely: 0.8 kW, 380 V, 3-phase, 50 Hz, 4 poles. SEIG is equipped with 26 μF capacitors that connected in Y. For two generators, testing scheme was used 405 W Energy-Saving Lamp (ESL) and Variabel Frequency Drive (VFD) as a non-linear load and resistor 900 Ω as other load. The both machines are rotated by the DC motor with a speed of 1536 rpm for SEIG and 1500 rpm for ISG in order to obtain the frequency and the terminal voltage reaches its nominal value. The measured machine parameter were: R_s = 8,20 Ω and X_s= 6,97 Ω for SEIG; R_s = 10,60 Ω for synchronous generator. And other parameters for both machines has been explained in Section 3 & 4.

The measurement of harmonic currents is carried out on three branch, namely: the non-linear load branch (**P1**), the other load branch (**P2**), and the stator windings branch (**P3**). In the meanwhile, the measurement of the harmonic voltages is performed at the **PCC** point. On this measure, the current flows in the branches of non-linear load measured in the direction of leaving the load. All testing of harmonic distortion is done using Power Analyzer CA 8220 that connected to PC.

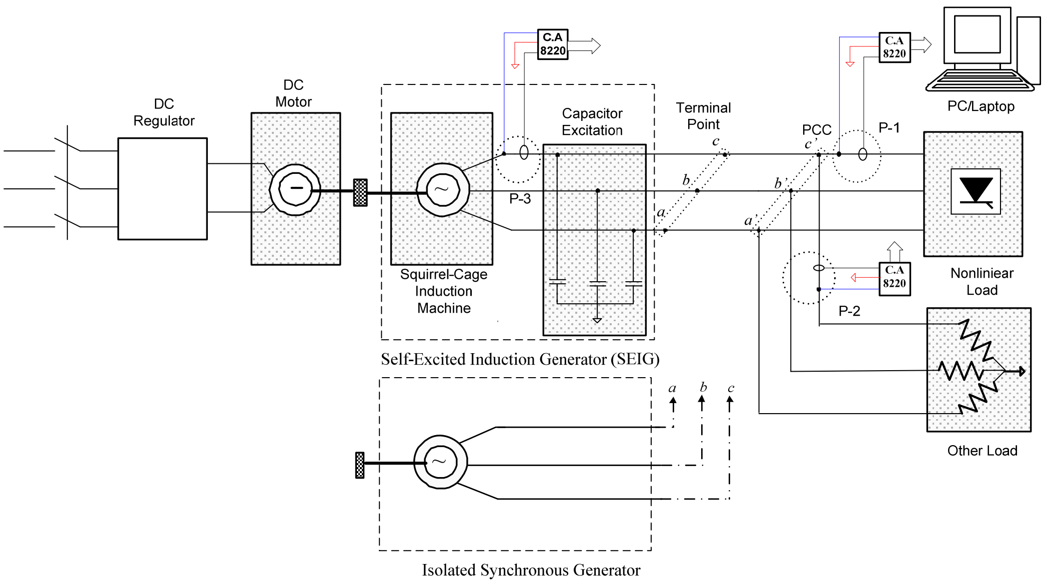

Figure 6. The testing circuit for all the proposed system

6. RESULTS AND DISCUSSIONS

6.1. The Harmonic Produced by The Non-linear Loads

Figure 7 show measurement results for the harmonics produced by non-linear load when SEIG encumbered with 405 W ESL. As shown by Figure 7a, the current waveform has deviated far from the ideal sinusoidal form because of harmonics effect, but the voltage waveform is almost close to the ideal sinusoidal form. This is in line the results shown by Figure 7b that THD_I and THD_V harmonic produced by ESL were 47.0% and 4.3% respectively. Figure 8 shows measurement results for the harmonics produced by non-linear load when SEIG encumbered with variable frequency drive (VFD). As shown by Figure 8, the value of THD_I will was greater (56.3%) when SEIG burdened with VFD. The component of harmonic currents scattered from low order to high order, wherein the component with the highest amplitude are on the order of 5,7,13.

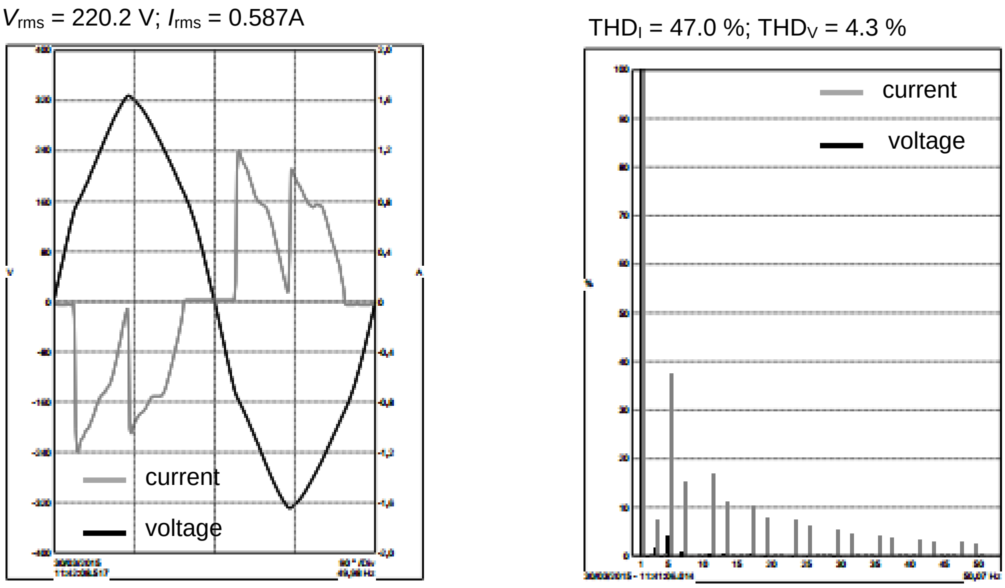

a. voltage and current waveform b. spectrum harmonic

Figure 7. The harmonic produced by non-linear load when SEIG burdened ESL

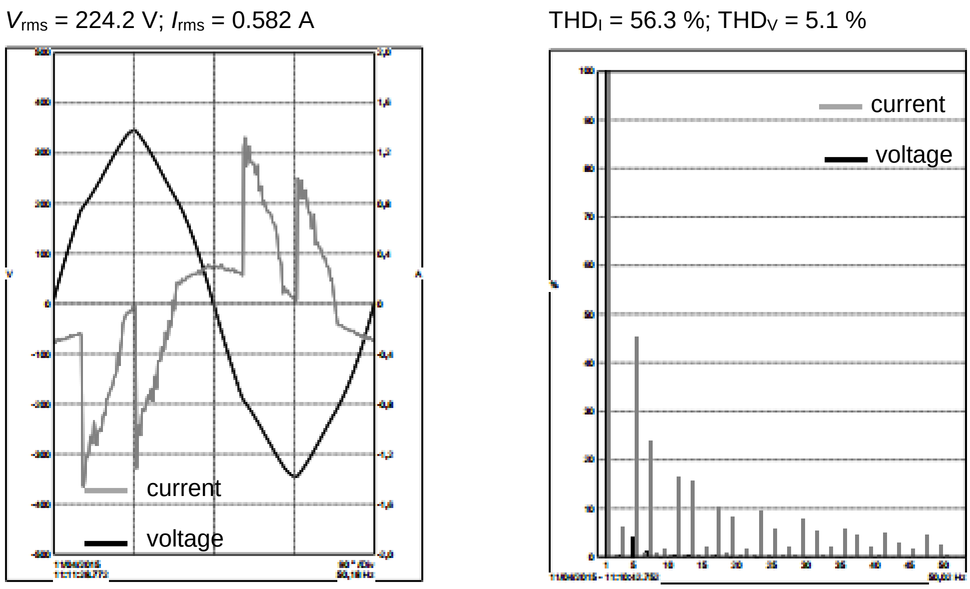

a. voltage and current waveform b. spectrum harmonic

Figure 8. The harmonic produced by non-linear load when SEIG encumbered with VFD

Figure 9 and 10 show measurement results for the harmonic generated by non-linear load when ISG encumbered with 405 W ESL and VFD respectively. As shown by these figure, THD_I for ISG was lower than SEIG, namely: 29.5 % (with ESL) and 24.2% (with VFD). However, THD_V was bigger when using ISG, namely: 13.7 % (with ESL) and 24.2% (with VFD). The Harmonics generated by ISG with non-linear loads more focused on low-order harmonic components, especially the order of 5 and 7.

The list of harmonic components produced by non-linear loads for both generators was used to analyze the harmonic distortion on stator side and other load using analysis method in section 3 & 4. The analysis results will be explained in next subsection.

V_{rms} = 221.4 V; I_{rms} = 0.524A THD_I = 29.5 %; THD_V = 13.7 %

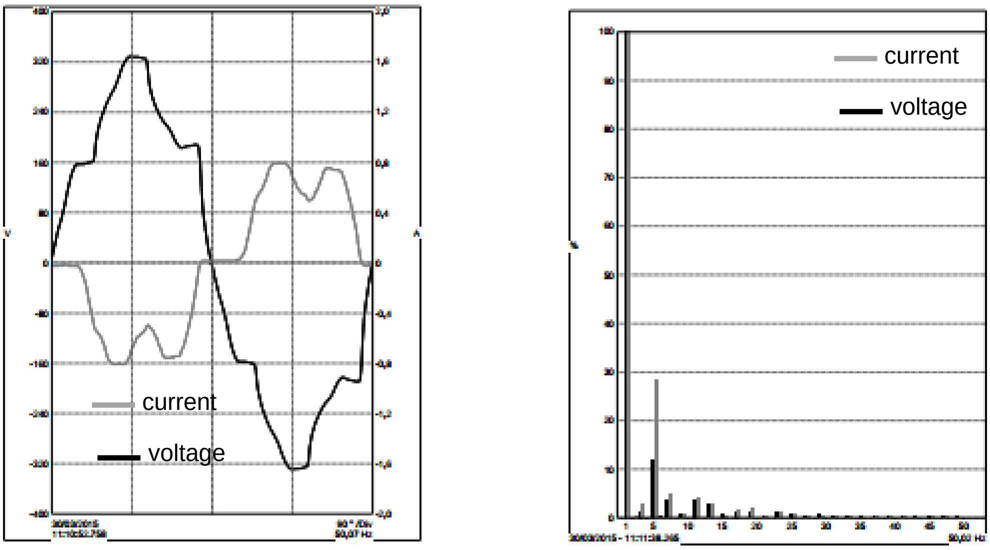

a. voltage and current waveform   b. spectrum harmonic

Figure 9. The harmonic produced by non-linear load when ISG encumbered with ESL

V_{rms} = 221.6 V; I_{rms} = 0.479A THD_I = 37.9 %; THD_V = 16.3 %

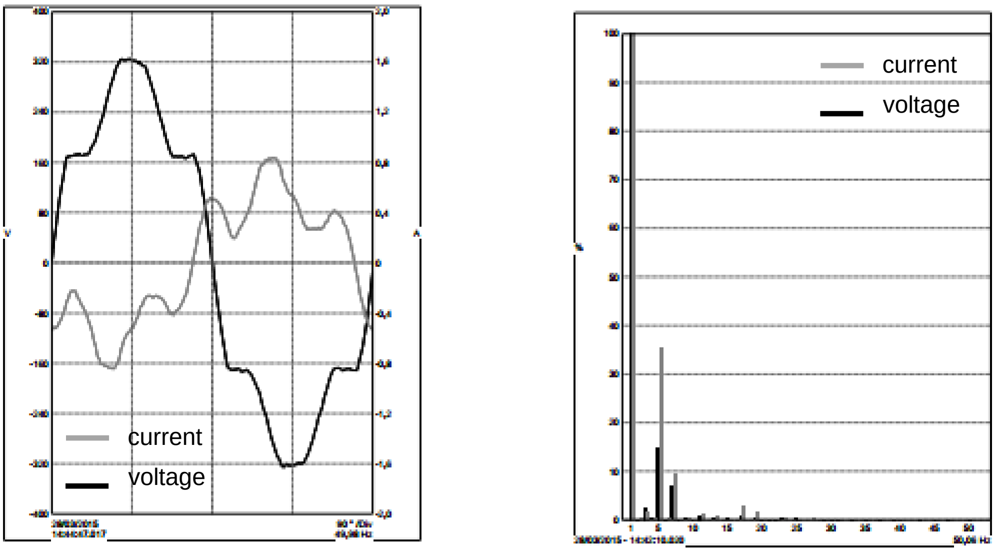

a. voltage and current waveform   b. spectrum harmonic

Figure 10. The harmonic produced by non-linear load when ISG burdened with VFD

6.2. The Impact of Non-linear Loads Against Harmonic Distortion on The Stator Windings

The impact of non-linear load on both generators can be measured from the level of harmonic distortion for the current of stator windings. Figure 11 and 12 show the current and voltage harmonic distortion on stator windings side and terminals when SEIG and ISG burdened with 405W ESL respectively. As shown these figure, THD_I & THD_V of the current stator windings and the terminals voltage of SEIG was lower than THD_I & THD_V level for ISG. The SEIG has eliminated almost all the harmonic components, except the harmonic component order 3th, 5th, and 7th. While, the stator current of ISG still has contained 3th, 5th, 7th, 11^{t}h, 13th, 17th and 19th order harmonic component.

THD_I = 10.1 %; THD_V = 4.1 %

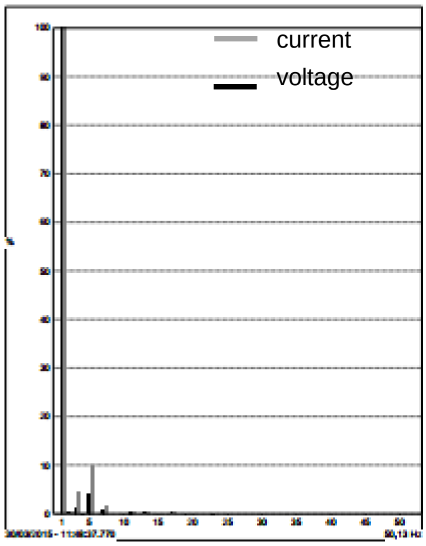

harmonic orders (h)

a. measured

THD_I = 8.05 % ; THD_V= 3.23%

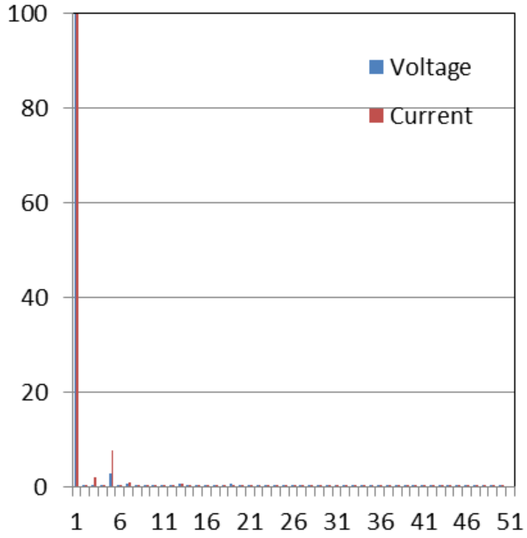

harmonic orders (h)

b. analyzed

Figure 11. The current harmonic distortion on the stator windings when SEIG burdened with ESL

THD_I = 17.80 %; THD_V = 14.0 %

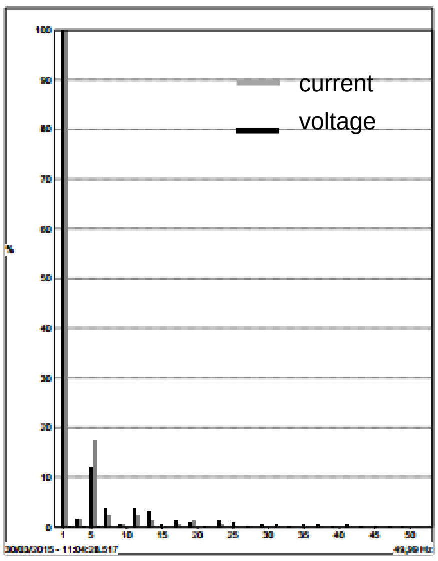

harmonic orders (h)

a. measured

THD_I = 17.25 %; THD_V=16.92%

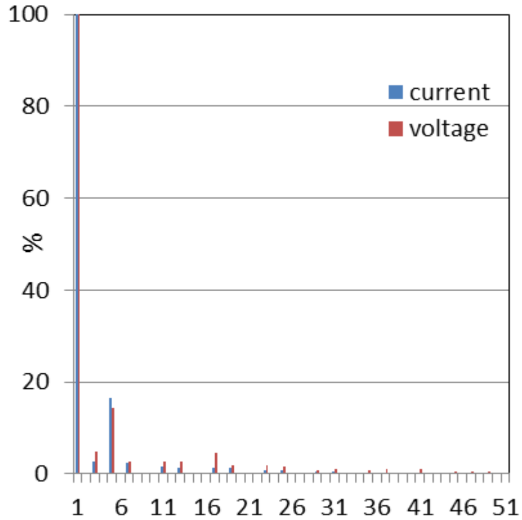

harmonic orders (h)

b. analyzed

Figure 12. The current harmonic distortion on the stator windings when ISG encumbered with ESL

Figure 13 and 14 show the current harmonic distortion on stator windings side when SEIG and ISG burdened with VFD respectively. Like as loading the both generators with ESL, the current and voltage harmonic distortion of the stator windings and terminals for SEIG was lower than the current and voltage harmonic distortion of the stator windings and terminals for ISG.

6.3. The Impact of Non-linear Loads Against Harmonic Distortion on The Other Loads

The harmonic current produced by the non-linear load also propagate to the other load connected to the PCC point, so the other load current will also be distorted. Table 1 contained the value of odd harmonic components & THD on other load when both generators burdened by non-linear loads. As shown this table, the impact of non-linear load against the harmonic distortion on the other load for SEIG was better than ISG. The THD_I and THD_V on the other load for applied SEIG were lower than when applied ISG.

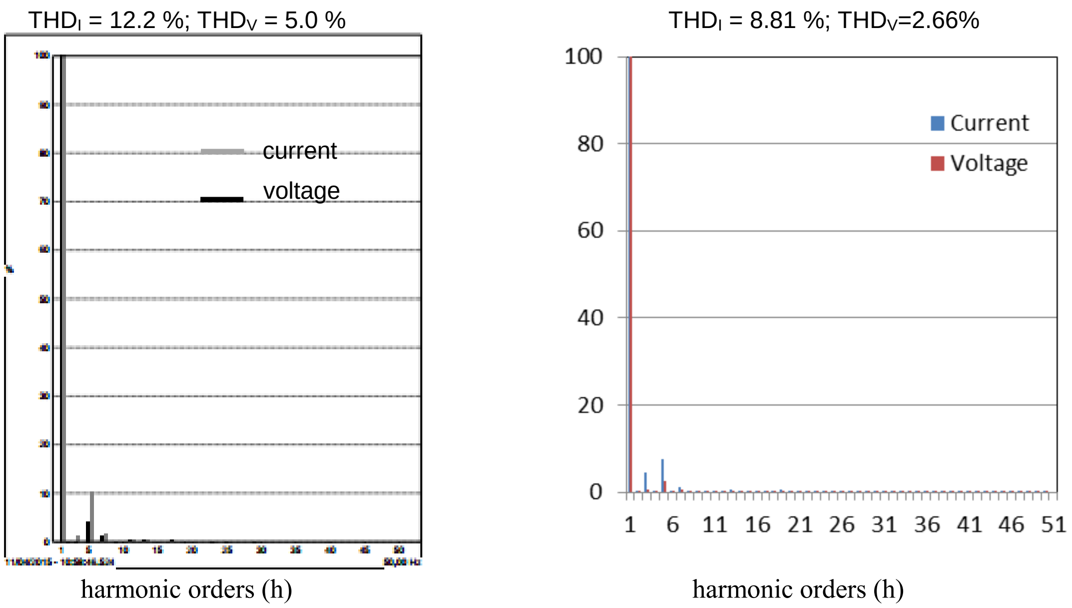

a. measured b. analyzed

Figure 13. The current harmonic distortion on the stator windings when SEIG encumbered with VFD

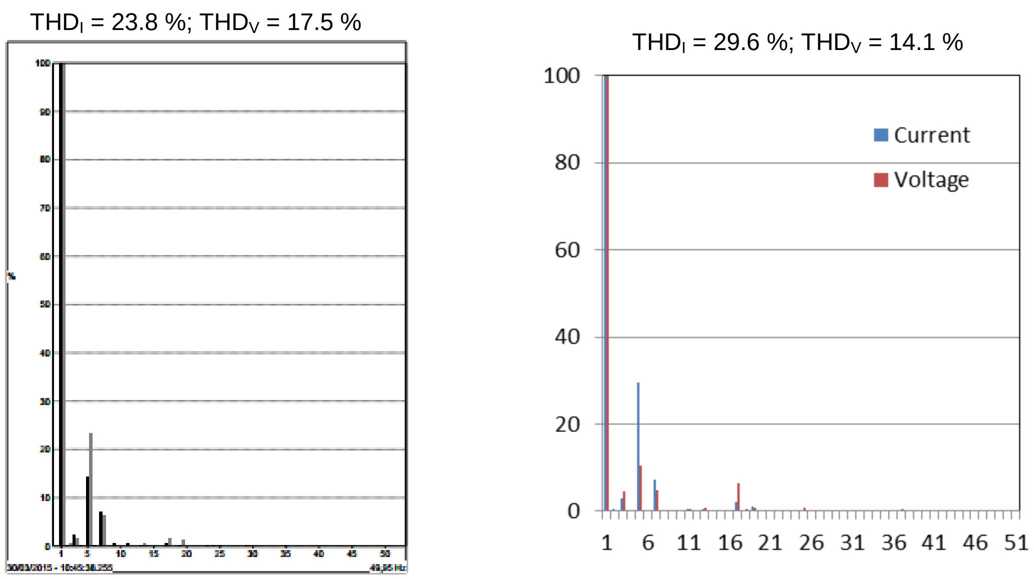

harmonic orders (h) harmonic orders (h)

a. measured b. analyzed

Figure 14. The current harmonic distortion on the stator windings when ISG encumbered with VFD

6.4. Discussion

As explained in section 6.1, the synchronous generator produced the harmonic current components fewer than SEIG, especially for high-order harmonic components. However, the harmonic distortion of PCC voltage on the synchronous generator was greater than SEIG. The harmonic currents generated by non-linear loads were depended on the generator impedance. The impedance of synchronous generator contains a large enough inductive reactance, which connected in series with non-linear loads (see Figure 1a.). For high order frequency, the reactance synchronous became large, so the harmonic components generated by non-linear load were reduced.

Tabel 1. The current odd harmonic components & THD on other load when the both generator burdened non-linear load

h	Measured (%)				Analyzed (%)			
	SEIG		Synchronous		SEIG		Synchronous	
	ESL	VFD	ESL	VFD	ESL	VFD	ESL	VFD
1	100.0	100.0	100.0	100.0	100.0	100.0	100.0	100.0
3	0.5	1.1	1.8	2.4	0.9	1.0	1.9	2.6
5	3.2	4.2	11.6	13.8	4.1	5.8	11.9	14.6
7	0.5	0.9	4.4	6.9	0.9	1.5	4.2	7.1
9	0.4	0.5	0.3	0.4	0.1	0.1	0.6	0.5
11	0.6	0.7	3.5	0.2	0.5	0.7	3.6	0.8
13	0.2	0.3	3.3	0.6	0.3	0.5	3.1	0.3
THD (%)	3.9	4.4	13.10	14.90	4.34	6.11	13.75	16.5

As described in section 6.2, the harmonics distortion of the stator windings current and terminal voltage was smaller when SEIG applied. This condition may occur due to a combination of the stator windings inductance and capacitor excitation may have eliminated the high-order harmonic currents and has attenuate the low-order harmonic currents on the stator windings. Moreover, because of the stator windings of synchronous generator is connected in series with the harmonic current source, then currents flowing in the stator windings was equal to the line current of synchronous generator. Furthermore, the low harmonic current distortion in the stator windings will be produced the minor harmonic deviations in the terminal voltage of SEIG..

As elaborated in section 6.3, the impact of the non-linear loads against the harmonic distortion on other loads connected to the same source will be better when used SEIG. The harmonic distortion on the other load is affected by two things, namely: the harmonic distortion on the terminal voltage and the current harmonics propagation of a nonlinear load.

7. CONCLUSION

This paper has presented and analysis the harmonic impact of non-linear load against the harmonic distortion on the generator windings and the other load connected to the same source. It proved the impact of non-linear load to the harmonic distortion on SEIG was smaller than ISG. The analysis results were verified by experiment results of laboratory testing. The harmonic current and voltage distortion in the stator windings of SEIG were lower than ISG. Furthermore, the harmonic current distortion effects on other loads connected in parallel to the terminals of SEIG was also lower than the other loads connected to ISG.

ACKNOWLEDGEMENT

Author would like thanks to Engineering Faculty, Andalas University for the financial support this work, through DIPA Funding (No. 014/PL/SPK/PNP/FT-Unand/2014).

REFERENCES

[1] Li Wang, Ping-Yi Lin, "Analysis of a Commercial Biogas Generation System Using a Gas Engine-Induction Generator Set", *IEEE Transactions on Energy Conversion*, vol/issue: 24(1), pp. 230-239, 2009.

[2] AM. Sayed, SM. Sharaf, SE. Elmasry, M. Elharony, "Dynamic Response of a Grid Connected Wind Farm with Different Types of Generators", *IJPEDS*, vol/issue: 2(1), pp. 85~98, 2012.

[3] Traine, "How VFDs Affect Genset Sizing", *Engineer News Letter*, vol. 35, 2006.

[4] Hashem Oraee Mirzamani, Azim Lotfjou Chobari, "Study of Harmonics Effects on Performance of In-duction Motors", 2005. www.wseas.us/elibrary/conferences/2005prague/Papers/493.

[5] IEEE Power Engineering Society, "IEEE Recommended Practices and Requirements for Harmonic Control in Electrical Power Systems", The Institute of Electrical and Electronics Engineers, Inc., 1993.
[6] Refdinal Nazir, "Analysis of Harmonic Currents Propagation on the Self-Excited Induction Generator with Nonlinear Loads", *Journal of Electrical Engineering & Technology*, vol/issue: 9(6), pp. 1935-1943, 2014.
[7] Ion Boldea, "The Electric Generators Handbook, Synchronous Generator", CRC Press Taylor & Francis, Boca Raton, 2009.
[8] A. Kusko, MT. Thompson, "Power Quality in Electrical System", Mc. Graw Hill, 2007.
[9] Stephen J. Chapman, "Electric Machinery Fundamentals", The McGraw Hill, 1999.
[10] Miloje Kostic, "Equivalent Circuit and Induction Motor Parameters for Harmonics Studies in Power Networks", *Eletrotehniski Vetstnik*, vol/issue: 79(3), pp. 135-140, 2012.
[11] Ion Daniel ILINA & Constantin GHIȚĂ, "Experimental Method for Estimating The Parameter of A Synchronous Machine Equivalent Scheme, wih Consideration of Skin Effect Influence", *U.P.B. Sci. Bull.*, Series C, vol/issue: 73(1), pp. 165-180, 2011.
[12] IEEE Power Engineering Society, "IEEE Standard Procedures for Obtaining Synchronous Machine Parameters by Standstill Frequency Response Testing", The Institute of Electrical and Electronics Engineers, Inc., 1987.

APPENDIX

The polynomial coeficient of machine parameters

i	SEIG			Synchronous Machines	
	e_i	c_i	d_i	k_i	m_i
1	0.019656014	8.05042818e-06	1.33095094e-07	0.000019106	0.000004881
2	-0.088230362	-0.00046874	7.88155364e-06	-0.000520051	-0.000180807
3	-0.013005548	0.01006005	-0.00017248	0.005088344	0.002307599
4	0.578249237	- 0.09657362	0.00168943	-0.022509893	-0.013318719
5	-	0.45742845	-0.00713447	0.239759872	0.177835792
6	-	3.72274449	0.02690408	-	-

BIOGRAPHIES OF AUTHORS

Refdinal Nazir received B.Eng. and M.T. degree in electrical engineering from Bandung Istitute of Technology, Indonesia, in 1985 and 1991 respectively, and Ph.D degree from University Technology of Malaysia in 1999. He is currently a senior lecture in Dept. of Electrical Engineering, Andalas University, Indonesia. His research interests are electric machines, renewable energy, distributed generation, and microgrid.

Krismadinata received the B.Eng. degree in electrical engineering from Andalas University, Padang, Indonesia, in 2000 and the M.Eng. degree from the Bandung Institute of Technology, Bandung, Indonesia, in 2004, and the Ph.D. degree from the University of Malaya, Kuala Lumpur, Malaysia, in 2012, and Post-doctoral at UMPEDAC within 2012-2014. He is currently with Dept. of Electrical Engineering, Universitas Negeri Padang, Indonesia. Dr. Kris has international patents and also as reviewer for many international journal in electrical engineering and energy fileds. His research interests are power electronics, control system and renewable energy.

Rizka Amalia, was born in Bukittinggi, West Sumatra, Indonesia in 1983. Received B.Eng. degree in electrical engineering from Andalas University, Indonesia, in 2006. From 2003 to 2006 active as an assistant Electrical Energy Conversion Laboratory. She is currently master students in Andalas University, Indonesia.